Theoretical and experimental studies on cross-bridge migration during cell disaggregation

Aydin Tozeren,* Kuo-Li Paul Sung,‡ and Shu Chien‡§
*Department of Mechanical Engineering, The Catholic University of America, Washington, DC 20064; ‡Department of Physiology and Cellular Biophysics, College of Physicians and Surgeons, Columbia University, New York 10032; and §Institute of Biomedical Sciences, Academia Sinica, Taipei, Taiwan 10529

ABSTRACT A micromanipulation method is used to determine the adhesive energy density (γ) between pairs of cytotoxic T cells (F1) and their target cells (JY: HLA-A2-B7-DR4,W6). γ is defined as the energy per unit area that must be supplied to reduce the region of contact between a conjugated cell pair. Our analysis of the data indicates that the force applied by the micropipette on the cell is not uniformly distributed throughout the contact region as we had previously assumed (Sung, K. L. P., L. A. Sung, M. Crimmins, S. J. Burakoff, and S. Chien. 1986. *Science (Wash. DC)*. 234:1405–1408), but acts only at the edges of the contact region. We show that γ is not constant during peeling but increases with decreasing contact area of the conjugated cell pairs F1-JY, F1-F1, and JY-JY in contrast to the constancy of γ for typical engineering adhesives. This finding supports the notion that the cross-linking protein molecules slide towards the conjugated area across the leading edge of the separation while remaining attached to both cells. Our mathematical analysis shows that the elastic energy stored in the cross-links by the membrane tensions balances the diffusive forces that act against cross-bridge migration. The binding affinity between F1-JY is found to be ~ 15–20 times larger than the corresponding affinity for F1-F1. The number of binding sites of F1 for attachment to JY is approximately the same for binding F1 to another F1 and vary between 10^5 and 10^6.

1. INTRODUCTION

Cell–cell adhesion plays an important role in tissue and organ development, cell-mediated immunity, and blood flow. Cells from different tissues display a hierarchy of adhesiveness that may stabilize the organization of cell layers during embryonic development (1–4). Red blood cell aggregation induced by macromolecules exerts complex effects on blood flow resistance and oxygen transport in vivo (5). In cell-mediated immunology, cytotoxic T cells specifically bind to and kill the target cells that activated them (1, 6). The first step of cell-mediated cytolysis is the conjugation of a human cytotoxic T lymphocyte with its specific target cell. The cell-to-cell adhesion could be a commitment step for cytolysis.

Recently, experimental and analytical methods have been introduced to quantify adhesive energy density between various cell pairs. The experimental methods involve either the shear disaggregation of two-cell aggregates in a flow chamber (5, 7–9), or separation of conjugated cell pairs by micromanipulating the holding pipettes (6, 10–12). Mechanics of adhesion and peeling have been extensively investigated in engineering and biomaterials literature by using the methods of interfacial chemistry, fracture of composites, and thermodynamics (13–17). This existing literature was utilized recently in the elegant models of red blood cell aggregation and rouleoux formation (18–21). In these models the specific binding due to cross-bridges were not considered.

Significant progress have also been made in modeling the micromechanics of cell adhesion (22–26). Bell et al. (23) and Bongrand and Bell (24) have developed a thermodynamic calculus for studying the competition between nonspecific (electrostatic) repulsion and specific binding. This model was then used to predict the contact area and the number of bridges between conjugated cell pairs after the process of adhesion reached equilibrium. More recently, Evans (25, 26) investigated the coupling between micromechanics of cell adhesion and the continuum equations of the adhering cell membranes. Evans (26) introduced the concept of kinetically trapped (stationary) cross-bridges and provided an explanation of the micromanipulation data (10) on erythrocyte aggregation in the presence of wheat germ agglutinin (WGA). These experiments show that negligible levels of tension are induced by adhesive contact even though the tension to separate the contact is large enough to rupture the membrane.

These aforementioned studies provide a valuable basis for our study of seperation of a conjugated cytotoxic T cell (human clone F1, with specificity for HLA-DR_{w6}) from its target cell (JY: HLA-A2,-B7,-DR4,w6). In the following section we describe briefly the micromanipulation method used in our experiments. The experimental method and some of the data used in the present analysis were published previously (6). However, for the present paper, we had to study the videotapes of Sung et al. (6) to determine the geometric parameters of adhesion and

0006-3495/89/03/479/09 $2.00

disaggregation for a set of pairs of cytotoxic cells (F1) and their target cells (JY). These experimental parameters and the aforementioned videotapes were not published previously.

In section 3 we discuss how to evaluate the adhesive energy density (γ) from experimental data. The analysis follows closely the recent study of Evans and Leung (10) on the disaggregation of red blood cell aggregates in the presence of WGA. We show that γ increases with the extent of peeling of conjugated cell pairs. This finding supports the notion that the cross-linking protein molecules slide towards the conjugated area while remaining attached to both cells.

In section 4 we introduce a model for the micromechanics of cell adhesion. In the model, it is assumed that the elastic energy stored in the cross-bridges by the membrane tensions can overcome the opposing diffusive and frictional forces and lead to cross-bridge migration. The model can be used to study the transient and steady-state phases of conjugation and disaggregation of cell pairs. One of the significant results of our analysis is the prediction that $1/\gamma$ is a linearly increasing function of the area of conjugation A_c (Eq. 15) for conjugation at equilibrium. This prediction is in excellent agreement with our experimental data obtained at small rates of peeling. It is shown that the slope and the intercept (A_c) of this straight line are functions of the initial cross-bridge density and the binding affinity of a cross-bridge attached with zero elastic strain. This model is used in the last section to deduce the biophysical properties of cross-bridges from experimental data.

2. METHODS

We describe below the micromanipulation method used in experiments on the disaggregation of a cytotoxic T cell from its target cell. The biochemical manipulations used in the experiments were reported in reference 6. In micromanipulation experiments, each cell was held at the tip of a micropipette by using a small aspiration pressure, and the cells were brought together and aligned by manipulating the holding pipettes. The aspiration pressure was then removed from the pipette holding the smaller cytotoxic T cell (cell 1) so that it could interact freely with the larger target cell (cell 2) still held by its pipette. About 10 min after the beginning of the conjugation, the cytotoxic T cell was recaptured with its pipette by the application of a small aspiration pressure. After cell 1 was recaptured, the aspiration pressure was increased stepwise at increments on the order of 100 dyn/cm^2. At each pressure level the pipette holding the cell was pulled away gradually by micromanipulation. When the aspiration pressure was low, such pulling caused the cytotoxic T cell to slip out of its holding pipette while remaining conjugated with the target cell. With sufficiently high pressures, the two cells could be separated completely as the pipette holding the cell 1 was being pulled away from the target cell. During this manipulation each cell remained attached to its holding pipette.

The 10-min incubation period was chosen because the area of conjugation reached its maximum during this period. The duration of 10 min is short enough to avoid the occurrence of cytolysis during separation. The results of the experiment did not change when the incubation time was lengthened to 15 min.

The minimum aspiration pressure that led to the total separation of the two cells was referred to as the critical separation pressure (P_{cr}). The critical seperation stress was then defined as the axial force exerted by the pipette on the cytotoxic T cell divided by the initial area of contact between two cells before the cells were pulled apart. The parameter S_c was computed by using the equation

$$S_c = 2\,(R_p/R_i)^2\,P_{cr}, \tag{1}$$

where R_p is the radius of the pipette holding the cell 1 and R_i is the radius of the interface of conjugation at rest. Sung et al. (6) computed S_c for a set of pairs of a cytotoxic T cell (F1) and its target cell (JY) and found it to be in the order of 10^4 dyn/cm^2.

A close study of the sequences of photographs taken from the video playback of the micromanipulation events indicates that the peeling of the two cells does not occur instantaneously but gradually with time (Fig. 1). Therefore the force exerted by the pipette in the direction of its axis (F_p^1) produces work only at the edges of the conjugated region. This process of separation is similar to the peeling of two adhesive tapes. For this reason we have reinvestigated the mechanics of separation of conjugated cell pairs (F1-JY, F1-F1, JY-JY). We have studied the videotapes of Sung et al. (6) which were not published in reference 1 and determined the geometric parameters of separation for a set of experiments involving cell pairs F1-JY, F1-F1, and JY-JY. These parameters will be introduced in the next section to compute the adhesive energy density (γ) from experimental data.

3. MACROSCOPIC ANALYSIS OF MICROMANIPULATION DATA

In continuum mechanics the breaking of the adhesive bond between two surfaces are usually characterized by introducing the concept of adhesive energy density γ (13–16). It is assumed that an energy density γ (dynes per centimeter) must be supplied to break a unit area of adhesive. The work done per unit area by the membrane tensions T_c^1 and T_c^2 during peeling of two tapes is then equal to the surface energy density γ, resulting in the following equation:

$$\gamma = T_c^1(1 - \cos\phi_1) + T_c^2(1 - \cos\phi_2), \tag{2}$$

where ϕ_1 and ϕ_2 are the angles the tapes make with the surface of contact, as shown in Fig. 2. Eq. 2 is the classical Young equation applied to the peeling of two adhering tapes. This equation may also be used to study the mechanics of peeling of conjugated cell pairs if the cell disaggregation proceeds by peeling at the edge of the contact region and that the speed of peeling is small enough to neglect the viscoelastic response of the cell interior. In such cases ϕ_1 and ϕ_2 denote, respectively, the angles cell 1 (F1) and cell 2 (JY in F1-JY, F1 in F1-F1) make with the surface of the contact, assumed to be a plane. T_c^1 and T_c^2 are the membrane tensions along the meridional direction at the rim of the contact.

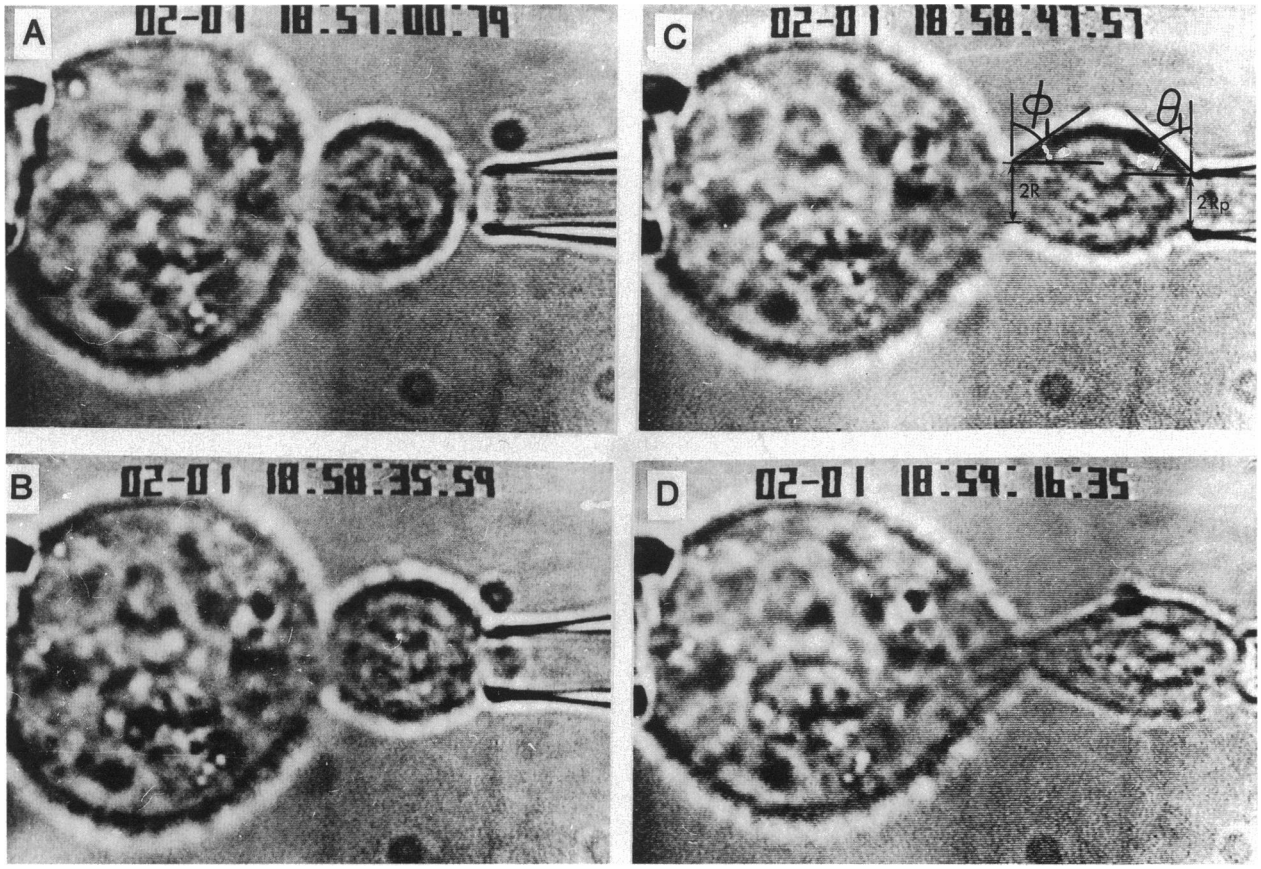

FIGURE 1 A sequence of photographs taken from the video monitor illustrating the time course of separation of a conjugated F1-JY pair. Parameters shown in the figure are used to compute the adhesive energy density γ defined in the text.

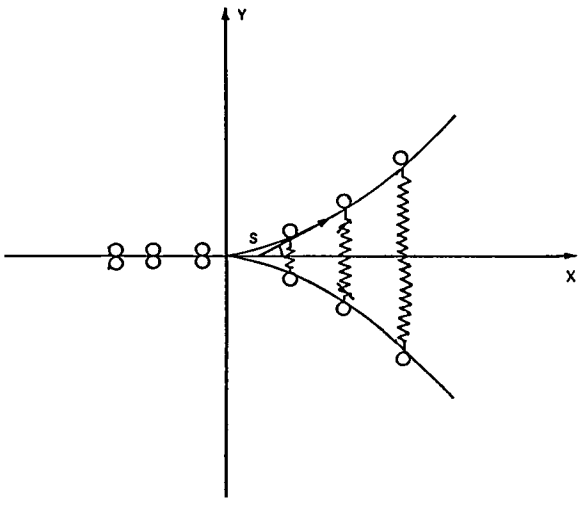

FIGURE 2 Schemmatic diagram illustrating the symbols used in analysis.

Membrane tensions T_c^1 and T_c^2 can be evaluated by considering the static equilibrium of the cell segment between the micropipette and the region of conjugation (10):

$$T_c^1 = P[R_p^2/(2R)][\sin\theta_1/\sin\phi_1] - (P_c - P_1) \cdot \{[R_p^2/(2R)](1 - \sin\theta_1) - (R/2)\}/\sin\phi_1, \quad (3)$$

where R is the radius of the area of conjugation and θ_1 is the angle cell 1 makes with the radial direction at the tip of the pipette (Fig. 1). P_c is the uniform pressure in the cell, P_1 is the pressure exterior to the cell outside the pipette, and P is the pipette suction pressure measured in the experiments. If P_2 denotes the pressure in the pipette, then $P = P_1 - P_2$. A similar equation holds for T_c^2. The axial force exerted by the micropipette on the cell (F_p^1) can be computed by considering the static equilibrium of the cell segment that lies in the pipette (10).

$$F_p^1 = \pi(R_p^2)[(P)\sin\theta_1 - (P_c - P_1)(1 - \sin\theta_1)]. \quad (4)$$

In the figures presented below, we have computed γ and

F_p^1 by using Eqs. 2–4 with $P_o = (P_c - P_l) = 0$. The justification for this and other assumptions used in determining γ from experimental data is presented in the Appendix. Fig. 3 shows γ as a function of A_c for typical F1-JY and F1-F1 pairs. The figure shows that γ increases with decreasing A_c as the two cells separate from each other. The increase in γ with the extent of separation is approximately 10-fold for F1-JY pair. For engineering adhesives, γ remains constant during peeling. It was difficult to estimate the values of $\theta_l$and ϕ_l from experimental data on JY-JY pairs for the range of A_c considered in Fig. 3, because A_c decreased rapidly to zero at the later stages of separation. The typical γ values obtained for JY-JY pairs at larger A_c are significantly smaller than the corresponding values for F1-F1 pairs.

We have next computed, using Eq. 4, the axial force F_p^1 as a function of the area of contact (A_c) for F1-JY and F1-F1 pairs. The results shown in Fig. 4 indicate that F_p^1 varies slightly as the peeling proceeds, but it is difficult to assess the limiting value of F_p^1 from the data shown in this figure, as A_c goes to zero.

The increase in the strength of adhesion during peeling may be due to the lateral migration of the cross-linking protein macromolecules through the plane of the membrane bilayer to a location where they may remain linked (5, 8, 10). In the next section we consider the possibility of cross-bridge migration during cell disaggregation in more detail.

4. MICROMECHANICS OF CELL ADHESION

In this section we develop a simple model of cell adhesion to relate the experimental adhesive energy density (γ) to the cross-bridge number density and the other biophysical parameters of the cross-bridges. For simplicity in presentation, we consider a conjugated pair of identical membranes with uniform thickness and width as shown in Fig. 2. The coordinates x and y and the arc length s are defined in the same figure. The (x,y) coordinate system is attached to the edge of separation and moves to the left during peeling. Arc length s is zero at the origin and increases from left to right. The force-free length is arbitrarily set equal to zero, so that twice the coordinate y represents the elastic extension in an attached cross-bridge.

The cross-bridge number density n ($1/nm^2$) is defined as the number of attached cross-bridges (bonds) per unit surface area. Similarly m ($1/nm^2$) denotes the corresponding density for unattached cross-bridges. In general m and n are functions of time t and arc length s. Next, we define the flux density parameters J_m and J_n as the rates of cross-bridge transport per unit length:

$$J_m = m\langle V_m\rangle, J_n = n\langle V_n\rangle, \quad (5)$$

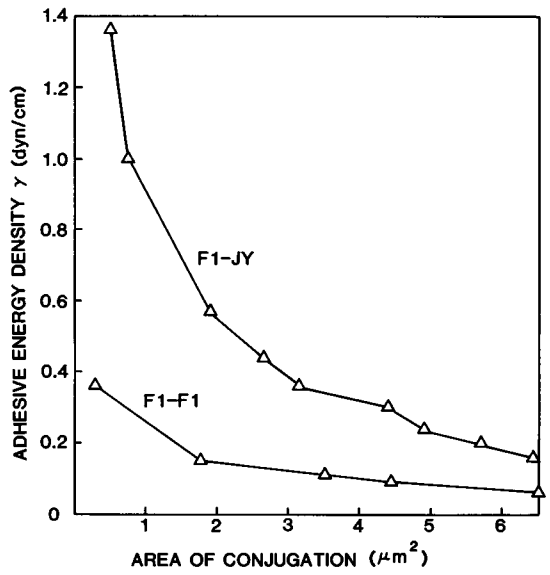

FIGURE 3 The variation of adhesive energy density γ with the area of conjugation (A_c) of typical cell pairs (F1-JY, F1-F1). Actual data points are connected by straight lines.

where $\langle V_m\rangle$ and $\langle V_n\rangle$ denote, respectively the average velocities of unattached and attached cross-bridges in the direction of increasing s (with respect to the (x,y) coordinate system). A cross-bridge flux can occur only in response to a force. Two distinct types of forces are assumed to contribute to the cross-bridge flux. The first is the elastic force in an attached cross-bridge which pulls the bond towards the remaining area of conjugation (to reduce the strain in the attached configuration). The

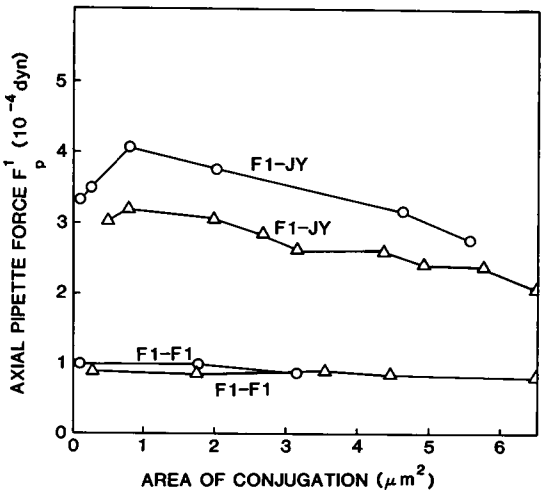

FIGURE 4 The variation of the axial pipette force F_p^1 with the area of conjugation (A_c) of the cell pairs (F1-JY, F1-F1). Actual data points are connected with straight lines.

second type of force is the diffusional force that tends to restore a uniform number density for the cross-bridges. Convective membrane flow due to endocytosis may also contribute to the flux density (27–29). However, this contribution was estimated to be negligible for small cells such as lymphocytes (27).

The flux parameters J_m and J_n can be assumed to be linear functions of the generalized forces on each component.

$$J_m - m\langle V_o\rangle = -D_{mm}(\partial m/\partial s) + D_{mn}(\partial n/\partial s) \quad (6a)$$

$$J_n - n\langle V_o\rangle = -D_{nn}(\partial n/\partial s) + D_{nm}(\partial m/\partial s) - n(K/f_n)(2y)(\partial y/\partial s), \quad (6b)$$

where V_o is the speed of peeling ($V_o > 0$), K (dyn/cm) denotes the cross-bridge stiffness in the attached configuration, D_{mm}, D_{nn}, D_{mn} and D_{nm} (nm^2/s) are the surface diffusion constants, and f_n (dyn-s/nm^2) is the frictional coefficient for the lateral mobility of the attached cross-bridges. Bell et al. (22) estimated K to be ~0.1 dyn/cm. The diffusion coefficients of various protein molecules in cell membranes have been measured by fluorescence photobleaching recovery technique (30, 31). These diffusion coefficients have a wide range of values varying between 5×10^{-9} to 10^{-12} cm^2/s. Such measurements (D_{mm}, D_{nn}) are not yet available for the molecules cross-linking a cytotoxic T cell to its target cell. A cross-bridge is expected to travel in the average a distance of ~ 11 μm during the ten-min incubation period if its diffusion coefficient is $\sim 5 \times 10^{-10}$ cm^2/s (27).

The diffusivity constants D_{nm} and D_{mn} describe how the flows of the two groups of cross-bridges interact and are related to each other by Onsager's reciprocity relationship (32). These cross terms are difficult to measure. They become negligible when cross-bridge interaction can be neglected. Under such conditions D_{mm} and D_{nn} can be expressed as (32):

$$D_{mm} = kT/f_m, D_{nn} = kT/f_n, \quad (7)$$

where k denotes the Boltzmann constant, T is the absolute temparature, and f_m is the friction coefficient for unattached cross-bridges.

The standard free energy functions (A_m, A_n of an unattached and an attached cross-bridge, respectively, are assumed to be

$$A_m = A_m^\circ \quad (8a)$$

$$A_n = A_n^\circ + K(y)^2, \quad (8b)$$

where A_m° and A_n° are constants. Cross-bridges are assumed to undergo a cycle of attachment and detachment governed by the following set of rate equations.

$$\partial m/\partial t + \partial J_m/\partial s = k_2 n - k_1 m \quad (9a)$$

$$\partial n/\partial t + \partial J_n/\partial s = k_1 m - k_2 n, \quad (9b)$$

where k_1 and k_2 (s^{-1}) are the rates of attachment and detachment, respectively. As in the sliding filament model of muscle contraction, k_1 and k_2 are assumed to be functions of the cross-bridge extension (33, 34). These rate functions are not assigned arbitrarily, but are assumed to satisfy the condition of detailed balance, namely (34):

$$k_1/k_2 = \exp\{[(A_m^\circ - A_n^\circ) - K(y)^2]/kT\}. \quad (10)$$

An exact solution to the cross-bridge density distribution can be obtained by combining Eqs. 6, 9 and 10.

$$n = n_c\{\exp[-(K/kT)y^2]\} \quad (11a)$$

$$m = n_c/b, \quad (11b)$$

where $b = \exp[(A_m^\circ - A_n^\circ)/kT]$, and n_c is the uniform density of attached cross-bridges in the conjugated area ($y = 0$). This solution corresponds to the following conditions: (*a*) The cross terms in the flux equation can be neglected ($D_{mn} = D_{nm} = 0$). (*b*) The speed of peeling is zero ($V_o = 0$). (*c*) Flux parameters are equal to zero ($J_m = J_n = 0$). (*d*) Steady state is reached ($dm/dt = dn/dt = 0$). These conditions are not exactly valid for the slow separation of conjugated cells considered here, but are reasonable because our experiments show that γ is not rate dependent for slow speeds of peeling considered here ($V_o = 0.004$ m/s).

Noting that the total number of attached and unattached cross-bridges in a cell membrane must remain constant during conjugation, n_c can be determined as a function of the initial cross-bridge density before adhesion (m_o).

$$n_c = m_o(b)/[1 + b(A_c/A_o)], \quad (12)$$

where (A_c/A_o) is the ratio of the conjugated surface area to the total surface area of the membrane.

Next, we consider the equations of equilibrium of the membrane along the arc length s and x directions, respectively (21, 25).

$$dT_1/ds = (n)(K)(2y)(dy/ds) \quad (13a)$$

$$T_c = (T_c^1)\cos(\phi_1), \quad (13b)$$

where T_1 denotes the membrane tension (dyn/cm), T_c is the uniform tension in the conjugated area ($y = 0$), and T_c^1 and ϕ_1 are the tension and the angle of inclination far from the edge of separation.

The bending resistances of the adhering cell membranes were not taken into account in deriving Eq. 13. In general, Eq. 13a (tangential force balance) should include an additional term on the right hand side due to the bending rigidity of the membrane (transverse shear stress

multiplied by the local meridional curvature) (21). A support for neglecting this term was provided by Burridge and Keller (15), who have analyzed the peeling of a beam from a plane to which it adheres. They showed that the classical Young equation is valid even in the presence of significant bending stresses. A similar conclusion was reached by Evans (25) recently in his continuum model of cell adhesion. The analysis provided here may not be entirely valid at the edge of contact where the membrane curvature undergoes significant changes due to unfolding during the course of peeling. We have also not taken into account the nonspecific repulsive forces in equations of membrane equilibrium (13). Our model can be generalized to include the effects of nonspecific repulsion by using the analysis developed by Bell et al. (23).

Eqs. 11–13 can be combined to yield the following equation:

$$T_c^1[1 - \cos(\phi_1)] = m_o(kT)b/[1 + b(A_c/A_o)]. \quad (14)$$

The term on the left-hand side can be shown to be equal to $\gamma/2$ by using Young's equation (2). The present analysis shows that γ increases with decreasing conjugated area when the bonds are allowed to migrate towards the remaining area of conjugation in a peeling membrane. Eq. 14 can be put in a more convenient form for determining parameters b and m_o from experimental data.

$$(1/\gamma) = [1/(2kTbm_o)] + [1/(2kTm_oA_o)]A_c. \quad (15)$$

The parameters γ and A_c can be evaluated from micromanipulation data as a function of time during peeling. The slope and the intercept ($A_c = 0$) of the experimental data can then be used to compute m_o and b. A lower bound for the surface area A_o of a cytotoxic T cell can be determined approximately from the micrograph shown in Fig. 1 by assuming a spherical geometry. In the next section we shall determine m_o and b for conjugated pairs of cytotoxic T cells and their target cells by using micromanipulation data.

5. EVALUATION OF CROSS-BRIDGE PARAMETERS

The aim of the present study is to quantify the strength of adhesion between a cytotoxic T cell (human clone F1, with specificity for HLA-DR_{w6}) and its target cell (JY: HLA-A2,-B7,-DR4,w6) before the delivery of lethal hit. The separation of cell pairs F1-F1 and JY-JY were studied as controls. This allows us to determine whether the junction avidity for F1-JY pairs is greater than those for F1-F1 and JY-JY pairs. We have shown in section 3 that the adhesive energy density γ, computed by using the classical Young equation, increases with the extent of separation. In section 4 we have introduced a model of cell adhesion to explain this observation and deduce the intrinsic parameters of adhesion from experimental data. In this model, we have allowed the migration of attached cross-bridges towards the conjugated area across the leading edge of separation. In this lateral migration, the elastic cross-bridge forces overcome the opposing viscous and diffusive forces. Each of the cross-linking protein macromolecules would then behave in a manner similar to the sliding tab of a zipper which makes peeling possible without necessarily breaking the structure. Hence, the work done by the cell membrane at the rim of the conjugated region may be used, in appropriate situations, not to break the cross-bridges but to overcome the frictional and diffusive forces that oppose the radially inward motion of the cross-bridges in the conjugated area. If the cross-bridges were not able to slide towards the area of conjugation, peeling would have to occur by the detachment of cross-bridges with an essentially uniform cross-bridge density, thus leading to a constant γ as observed in most engineering adhesives. Note also that in the model we have assumed a cross-bridge cycle of attachment and detachment. This means that not all attached cross-bridges remain attached during migration towards the area of conjugation.

According to the model (Eq. 15) $1/\gamma$ must be a linearly increasing function of the area of conjugation (A_c). The slope and area intercept of this line were shown to be equal to $[1/(2kTm_oA_o)]$ and $[1/(2kTbm_o]$, respectively. A_o denotes the uniform density of cross-bridges on a free F1 cell, and the dimensionless binding affinity b is defined in Eq. 11. In Fig. 5 we have plotted the experimental values of $(1/\gamma)$ vs. A_c for typical cell pairs F1-JY and F1-F1 (discrete points in the figure). The figure shows that the dependence of $(1/\gamma)$ on A_c is reasonably linear in accordance with the model predictions (*solid lines*). The model predictions shown in Fig. 5 correspond to $m_o = 1/(2{,}400\ \text{nm}^2)$ and $b = 1{,}500$ for F1-JY pairs, and $m_o = 1/(1{,}900\ \text{nm}^2)$ and $b = 80$ for F1-F1 pairs. In the computations for m_o and b, we have assumed that $kT = 4.1 \times 10^{-14}$ dyn-cm ($T = 25°C$), and $A_o = 360\ \mu\text{m}^2$. In the estimation of the total membrane area, the excess surface area of the cell present in the form of folds was assumed to be equal to the surface area determined by assuming a smooth spherical geometry (35). Berke (36) had found previously a number density of $1/(2{,}000\ \text{nm}^2)$ for conjugates of cytotoxic T cells and their target cells. Our findings agree very closely with this estimate. These results show that the number of receptor sites bridging F1 to JY is approximately the same as the number of links bridging F1 to F1, and the binding affinity between F1 and JY is ~ 15–20 times larger than the corresponding affinity between two F1 cells.

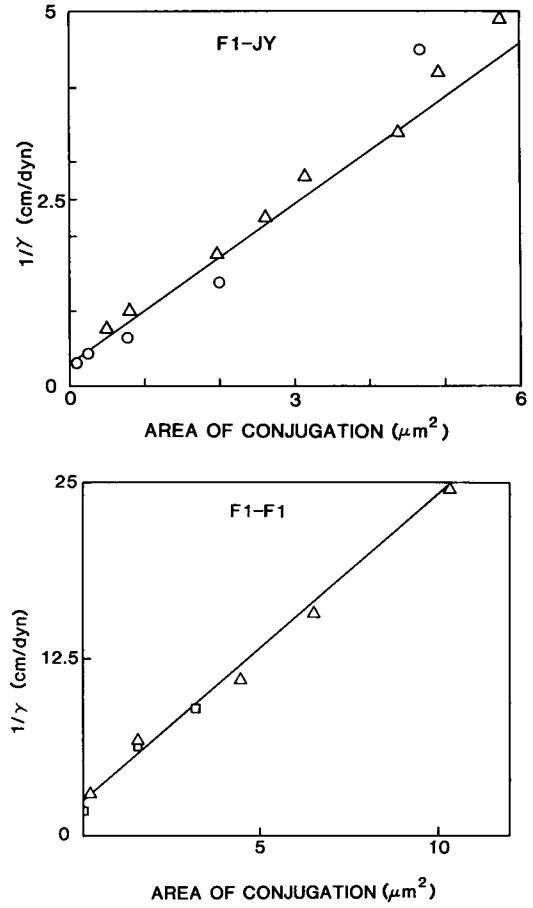

FIGURE 5 The variation of $(1/\gamma)$ with the area of conjugation (A_c) for two sets of cell pairs F1-JY (*A*) and F1-F1 (*B*). γ is the adhesive energy density (dyn/cm). The discrete points correspond to the micromanipulation data presented in Fig. 4. The different symbols in the figure correspond to different pairs of cells. Continuous straight lines show the model predictions (Eq. 15) obtained with the following parameter values: $A_o = 360\ \mu m^2$ and $kT = 4.1 \times 10^{-14}$ dyn-cm for F1-JY and F1-F1, $m_o = 1/(2{,}400\ nm^2)$ and $b = 1{,}500$ for F1-JY; $m_o = 1/(1{,}900\ nm^2)$ and $b = 80$ for F1-F1.

Our results (Eq. 14) indicate that the cross-bridge stiffness (K) influences the cell membrane curvature at the leading edge of separation, but has little influence on γ. With K increasing, the cross-bridges will break most likely at lower levels of strain, but that the energy required for peeling will not change. However this result may be due to the integration of membrane equilibrium equations for attached cross-bridge extensions in the range $(0 < y < \infty)$. γ will depend on K if an upperbound is assumed to exist for cross-bridge extension.

Our experimental data and Eq. 12 show that the cross-bridge density at the area of conjugation increases by an order of magnitude during the course of separation for F1-JY pairs. It is then possible that the friction coefficients f_m and f_n may increase due to the crowding of macromolecules at the region of conjugation. Under these conditions it would be more difficult for the cross-bridges to move to a less strained position before detachment. Hence it would be expected that the links will likely break rather than slide at sufficiently high membrane tensions.

Many membrane proteins are known to be restricted in their lateral mobility by barriers such as tight junctions. Our experimental data show that γ is bound as A_c goes to zero. Hence in our model no barrier exists between the contact region where cross-bridges attach with zero strain and the edge of this zone. The cross-bridges that migrate toward the leading edge of separation can diffuse freely into the region of conjugation.

Our experiments show that adhesion-separation process is repeatable. It is therefore reasonable to assume that significant amounts of cross-linking between attached cross-bridges do not occur in our experiments. Our model predicts correctly that the conjugation will recover back to its initial maximum value if the external pipette force on cell 1 is released at any time during separation. This is because the membrane tensions after the release are not large enough to store sufficent elastic energy into the cross-bridges at the leading edge of separation which could balance the diffusive forces. The diffusive forces act to create a uniform cross-bridge number density throughout the cell surface.

In the model developed in section 4, we have considered, for simplicity, the peeling of two identical membranes. The model would become much more complex if one allowed for different diffusive and rheological coefficients for each membrane. If the cells are not identical, attached cross-bridges do not necessarily remain perpendicular to the surface of conjugation. Hence the cross-bridge orientation, along with the cross-bridge number density, must be computed as a function of position. Additional equations would then be required to govern the evolution of cross-bridge orientation during cell separation.

We have made a set of reasonable approximations in evaluating the adhesive energy density as a function of the extent of separation and deduced from this relationship the intrinsic parameters of adhesion. Our experimental observation that γ increases with the extent of separation has been shown for other types of cells by using different experimental methods (5, 6, 10). The model discussed in section 4 is a mathematical formulation of a mechanism for cross-bridge migration consistent with the aforementioned data. This model can be used to estimate the values of the intrinsic parameters such as b and m_o from micromanipulation data. This study is considered to be an attempt to bridge the gap between the micromechanics of cell adhesion, the macroscopic data, and the classical analysis of peeling.

APPENDIX

In this appendix we discuss the assumptions made in evaluating the adhesive energy density from micromanipulation data. First, we have assumed that the pressure in the cell (P_c) is approximately equal to the pressure exterior to the cell outside the pipette (P_1). Hence, we set $P_o = (P_c - P_1) = 0$ in Eqs. 3 and 4. In cells with excess membrane in the form of folds, the circumferential tension in the membrane will be small and therefore P_o can be neglected (10). Electron micrographs of lymphocytes exhibit excess surface area in the form of folds (1, 35, 36), but these folds are not clearly discernable with the level of magnification that can be achieved in our micromanipulation experiments. T lymphocytes, during circulation between blood and lymph, squeeze through endothelial cells and undergo a considerable amount of deformation. The existence of excess cell membrane is instrumental in the ability of these cells to undergo large dimensional changes without significantly increasing the pressure in the cell.

The values of γ presented in Fig. 3 not only include the energy required to peel the cells, but also the work of unraveling the part of the membrane. It is expected that membrane tensions of ~0.05–0.1 dyn/cm will unravel these folds. Our data show that the membrane tension T_p^1 is slightly above this level at the initiation of seperation, but it increases at least by an order of magnitude for a typical F1-JY pair. Therefore the work density for unraveling membrane becomes small compared with γ in advanced stages of separation.

Analysis of separation of conjugated cell pairs would be more difficult if the cells involved in adhesion did not have excess surface area. The omission of $P_o = P_c - P_1$ would then become critical. It is difficult to evaluate P_o without considering the stress-deformation analysis of the entire cell. Elegant computational solutions of large deformation of cells under various loading conditions are becoming increasingly available in the literature (37–41). Ozkaya (40) considered the axisymmetrical flow of an erythrocyte through a narrow rigid tube and showed that the ratio of the internal cell pressure to the driving pressure (P_o/P) increased from 30 to nearly 40% as the driving pressure was increased > 10-fold, from 10 dyn/cm to 130 dyn/cm (see Table 9 and Fig. 63 in reference 40).

An upper bound for P_o that is valid for disaggregation of cells with no excess surface area can be obtained by assuming that the circumferential tension (T_2) be equal to the meridional tension (T_1) at any point in the membrane. It is usually expected that $T_2 < T_1$ when the membrane is stretched in the axial direction. The hydrostatic membrane stress distribution considered here could occur, for example, if the membrane tensions were single valued functions of area stretch. Using the condition of force balance along meridional direction, it can be shown that the membrane tensions are uniform throughout the cell membrane. The force balance in the direction normal to the membrane can then be used to obtain the following simple relation: $(P_c - P_1) = (R_p/R_o)(P_c - P_2)$, where $1/R_o$ is the mean curvature of the membrane that lies outside the pipette. In the following, we define α to be the ratio (R_p/R_o) at the location where the cell cross-section normal to the axis of the pipette is greatest. We have measured α from the sequences of photographs shown in Fig. 1. We found that $\alpha = 0.3$ for frame *A*, and $\alpha = 0.2$ for frame *D*. Next, we have computed γ by using Eqs. 2–4, but with $\alpha = 0.3$. Our computations showed that, at the initial stages of separation ($A_c = 6.4\ \mu m^2$), $\gamma = 0.08$ dyn/cm for $\alpha = 0$ and $\gamma = 0.15$ dyn/cm for $\alpha = 0.3$. For the final stages of separation ($A_c = 0.5\ \mu m^2$) we found that $\gamma = 0.68$ dyn/cm for $\alpha = 0$, and $\gamma = 0.63$ dyn/cm for $\alpha = 0.3$. These results show that γ increased with the extent of seperation even in the presence of considerable circumferential tension and absence of any excess membrane area.

Our experimental results indicate that ϕ_1 and ϕ_2 vary between 25° and 75° during the course of peeling, but that they are not necessarily equal to each other at all times. However, in the computations presented in section 3, we used the assumption that $T_c^1 = T_c^2$ and $\phi_1 = \phi_2$, because Θ_1 and ϕ_1 were more readily measurable from the sequences of photographs of the micromanipulation events. If two identical cells were involved in conjugation, γ values computed with this procedure would be equal to the actual adhesive energy density.

In Eqs. 2–4, we treated the cell interior as a fluid, because T cells contain very little rough endoplasmic reticulum which would contribute significantly to the cell stiffness, but are instead filled with easily flowing individual ribosomes. A further justification to this assumption can be found in Dong et al. (41). These authors modeled the cell interior of white blood cells as a Maxwell fluid with a time constant τ of ~ 1 s. A Maxwell fluid is an idealized viscoelastic material which behaves as elastic immediately after a sudden change in loading, but exhibits fluid behavior during slow loading or release. The aforementioned study shows that the viscous dissipation and inertia of the cells and the surrounding fluid can be neglected because the cell separation by micromanipulation is a slow event (2 min) compared with the time constant of cell interior (1 s).

This investigation was supported by National Science Foundation grant DCB-8719006 and National Institutes of Health grants GM4160 and HL16851.

Received for publication 16 May 1988 and in final form 7 November 1988.

REFERENCES

1. Alberts, B., D. Bray, J. Lewis, M. Raff, K. Roberts, and J. D.Watson. 1983. Molecular Biology of The Cell. Garland Publishing Inc., New York.
2. Townes, P., and J. Holfreten. 1955. Directed movements and selected adhesion of embryonic amphibian cells. *J. Exp. Zool.* 128:53–120.
3. Roth, S., and J. Weston. 1967. The measurement of intercellular adhesion. *Proc. Natl. Acad. Sci. USA.* 58:974–980.
4. Steinberg, M. S. 1970. Does differential adhesion govern self-assembly process in histogenesis? Equilibrium configurations and the emergency of a hierarchy among populations of embryonic cells. *J. Exp. Zool.* 173:395–434.
5. Chien, S., and L. A. Sung. 1987. Physicochemical basis and clinical implications of red cell aggregation. *Clin. Hemorheol* 7:71–91.
6. Sung, K. L. P., L. A. Sung, M. Crimmins, S. J. Burakoff, and S. Chien. 1986. Determination of junction avidity of cytotoxic T-cell and target cell. *Science.* 234:1405–1408.
7. Mohandas, N., R. M. Hocmuth, and E. E. Spaeth. 1974. Adhesion of red cells to foreign surfaces in the presence of flow. *J. Biomed. Mater. Res.* 8:119–136.
8. Vayo, M., R. Skalak, P. Brunn, S. Usami, and S. Chien. 1987. The role of the surface adhesive energy in shear dissagregation of red cell rouleaux. *Fed. Proc.* 46:1043.
9. Tha, S.P., J. Shuster, and H. L. Goldsmith. 1986. Interaction forces between red cells agglutinated by antibody. II. Measurement of hydrodynamic force of breakup. *Biophys. J.* 50:1117–1126.
10. Evans, E. A., and A. Leung. 1984. Adhesivity and rigidity of erythrocyte membrane in relation to wheat germ agglutinin in binding. *J. Cell Biol.* 98:1201–1208.

11. Evans, E., and K. Baxbaum. 1981. Affinity of red blood cell membrane for particle surfaces measured by the extent of particle encapculation. *Biophys. J.* 34:1–12.
12. Tha, S. P., and H. L. Goldsmith. 1988. Interaction forces between red cells agglutinated by antibody. III. Micromanipulation. *Biophys. J.* 53:677–687.
13. Gent, A. N., and G. R. Hamed. 1986. Bond strength: peel. *In* Encyclopedia of Materials, Science and Engineering. M. B. Bever, editor. Pergamon Press, New York. 373–378
14. Kaelbe, D. H. 1960. Theory and analysis of peel adhesion: Bond stresses and distributions. *Trans. Soc. Rheol.* 4:45–73.
15. Burridge, R., and J. B. Keller. 1978. Peeling, slipping and cracking: some one dimensional free-boundary problems in mechanics. *SIAM (Soc. Ind. Appl. Math.) Rev.* 20:31–61.
16. Anderson, G. P., S. J. Bennet, and K. L. DeVries. 1977. Analysis and Testing of Adhesive Bonds. Academic Press, New York. 286 pp.
17. Vogler, E. A. 1988. Thermodynamics of short-term cell adhesion in vitro. *Biophys. J.* 53:759–769.
18. Skalak, R., P. R. Zarda, K. M. Jan, and S. Chien. 1981. Mechanics of rouleaux formation. *Biophys. J.* 35:771–781.
19. Skalak, R., and S. Chien. 1982. Theoretical models of rouleaux formation. *Ann. NY Acad. Sci.*.
20. Evans, E., and V. A. Parsegian. 1983. Energetics of membrane deformation and adhesion in cell-vesicle aggregation. *Ann. NY Acad. Sci.* 416:13–33.
21. Evans, E., and R. Skalak. 1980. Mechanics and Thermodynamics of Biomembranes. CRC Press, Inc., Boca Raton, FL.
22. Bell, G. I. 1978. Models for the specific adhesion of cells to cells. *Science (Wash. DC).* 200:618–627.
23. Bell, G. I., M. Dembo, and P. Bongrand. 1984. Cell-cell adhesion: competition between nonspecific repulsion and specific bonding. *Biophys. J.* 45:1051–1064.
24. Bongrand, P., C. Capo, and R. Depieds. 1982. Physics of cell adhesion. *Prog. Surf. Membr. Sci.* 12:217–285.
25. Evans, E. A. 1985. Detailed mechanics of membrane–membrane adhesion and separation. I. Continuum of molecular cross-bridges. *Biophs. J.* 48:154–183.
26. Evans, E. A. 1985. Detailed mechanics of membrane–membrane adhesion and separation. II. Kinetically trapped molecular cross-bridges. *Biophys. J.* 48:185–192.
27. Goldstein, B., and F. W. Wiegel. 1988. The distribution of cell surface proteins on spreading cells. *Biophys. J.* 53:175–184.
28. Bretscher, M. S. 1984. Endocytosis: relation to capping and cell locomotion. *Science (Wash. DC).* 224:681–686.
29. Wiegel, F. W. 1979. Hydrodynamics of a permeable patch in the fluid membrane. *J. Theor. Biol.* 77:189–193.
30. Axelrod, D. 1983. Lateral motion of membrane proteins and biological function. *J. Membr. Biol.* 75:1–110.
31. Axelrod, D., D. E. Koppel, J. Schlessinger, E. Elson, W. W. Webb, and T. R. Podleski. 1976. Mobility measurements by analysis of fluorescence photobleaching recovery kinetics. *Biophys. J.* 16:1055–1069.
32. Cantor, C.R., and P. R. Schimmel. 1980. Biophysical Chemistry. II: Techniques for the Study of Biological Structure and Function. W. H. Freeman and Co., San Francisco, CA. 532 pp.
33. Huxley, A. F. 1957. Muscle structure and the theories of contraction. *Prog. Biophys. Biophys. Chem.* 7:255–318.
34. Hill, T. L. 1974. Theoretical formalism for the sliding filament model of contraction of striated muscle, part I. *Prog. Biophys. Mol. Biol.* 28:267–340.
35. Schmid-Schonbein, G. W., Y. Shih, and S. Chien. 1980. Morphometry of human leukocytes. *Blood.* 55:866–876.
36. Berke, G. 1983. Cytotoxic T-lymphocyte. How do they function? *Immunol. Rev.* 72:5.
37. Zarda, P. R., S. Chien, and R. Skalak. 1977. Interaction of a viscous incompressible fluid with an elastic body. *In* Computational Methods For Fluid-Structure Interaction Problems. T. Belytschko, and T. L. Geers, editors. American Society of Mechanical Engineers, New York. 41–48.
38. Daily, B., E. L. Elson, and G. I. Zahalak. 1984. Cell poking (determination of the elastic area compressibility modulus of the erythrocyte membrane). *Biophys. J.* 45:671–682.
39. Secomb, T. W., R. Skalak, N. Ozkaya, and J. F. Gross. 1986. Flow of axisymetrical red blood cells in narrow capillaries. *J. Fluid Mech.* 163:405–423.
40. Ozkaya, N. 1986. Viscous flows of particles in tubes: Lubrication theory and finite element models. Ph.D. thesis, Columbia University, New York.
41. Dong, C., R. Skalak, K. L. P. Sung, G. W. Schmid-Schoenbein, and S. Chien. Passive deformation analysis of human leukocytes. *J. Biomech. Eng.* 110:27–36.